



## Original paper

# Eye lens dose correlations with personal dose equivalent and patient exposure in paediatric interventional cardiology performed with a fluoroscopic biplane system



L. Alejo<sup>a,\*</sup>, C. Koren<sup>a</sup>, E. Corredoira<sup>a</sup>, F. Sánchez<sup>a</sup>, J. Bayón<sup>a</sup>, A. Serrada<sup>a</sup>, E. Guibelalde<sup>b</sup>

<sup>a</sup> Medical Physics Department, La Paz University Hospital, Madrid, Spain

<sup>b</sup> Radiology Department, Complutense University, Madrid, Spain

## ARTICLE INFO

## Article history:

Received 3 November 2016

Received in Revised form 16 March 2017

Accepted 20 March 2017

Available online 27 March 2017

## Keywords:

Eye lens dose correlations

Paediatric interventional cardiology

Biplane X-ray system

Optically stimulated luminescence

## ABSTRACT

**Purpose:** To analyse the correlations between the eye lens dose estimates performed with dosimeters placed next to the eyes of paediatric interventional cardiologists working with a biplane system, the personal dose equivalent measured on the thorax and the patient dose.

**Methods:** The eye lens dose was estimated in terms of  $H_p(0.07)$  on a monthly basis, placing optically stimulated luminescence dosimeters (OSLDs) on goggles. The  $H_p(0.07)$  personal dose equivalent was measured over aprons with whole-body OSLDs. Data on patient dose as recorded by the kerma-area product ( $P_{KA}$ ) were collected using an automatic dose management system. The 2 paediatric cardiologists working in the facility were involved in the study, and 222 interventions in a 1-year period were evaluated. The ceiling-suspended screen was often disregarded during interventions.

**Results:** The annual eye lens doses estimated on goggles were  $4.13 \pm 0.93$  and  $4.98 \pm 1.28$  mSv. Over the aprons, the doses obtained were  $10.83 \pm 0.99$  and  $11.97 \pm 1.44$  mSv. The correlation between the goggles and the apron dose was  $R^2 = 0.89$ , with a ratio of 0.38. The correlation with the patient dose was  $R^2 = 0.40$ , with a ratio of  $1.79 \mu\text{Sv Gy}^{-1} \text{cm}^{-2}$ . The dose per procedure obtained over the aprons was  $102 \pm 16 \mu\text{Sv}$ , and on goggles  $40 \pm 9 \mu\text{Sv}$ . The eye lens dose normalized to  $P_{KA}$  was  $2.21 \pm 0.58 \mu\text{Sv Gy}^{-1} \text{cm}^{-2}$ .

**Conclusions:** Measurements of personal dose equivalent over the paediatric cardiologist's apron are useful to estimate eye lens dose levels if no radiation protection devices are typically used.

© 2017 Associazione Italiana di Fisica Medica. Published by Elsevier Ltd. All rights reserved.

## 1. Introduction

Interventional cardiology (IC) is a medical speciality with high exposure to ionising radiation, both for patients and staff [1]. Although these procedures are minimally invasive and offer advantages over surgery for certain diseases, the development of new practices has led to an increased number and complexity of procedures in recent years, subjecting patients and operators to higher radiation doses than those encountered in general radiology [2]. There is increased interest in occupational doses to the professionals involved in these procedures since the April 2011 International Commission on Radiological Protection (ICRP) statement [3], which is covered by the new 2013/59 Euratom directive of December 5, 2013 [4]. This new European directive reduces the equivalent dose limit for the eye lens in planned occupational exposure situations from 150 to 20 mSv per year, averaged over 5-year periods, such

that doses of 50 mSv in a single year are not exceeded. This limit can be exceeded if radiation protection measures are not used in procedures performed on adult patients [5–7]. In paediatric IC, lower doses to child patients than to adult patients have recently been reported [8–10]; thus, lower doses in the exposed practitioners' eye lenses are expected, although longer interventions are typically observed and protective ceiling-suspended screens are often not used [12]. Although literature detailing the operational implications of applying this limit in paediatric patients is scarce, interest is growing [11,13,14].

Various dosimetric methods for estimating the dose to the lens are available, from personal dosimeters placed over the lead apron [15] to thermoluminescent dosimeters located at eye level [16]. Recent efforts have been made to evaluate various approaches to properly estimating the eye lens dose during interventional procedures, analysing the influence of both the type and position of the dosimeter [17]. Likewise, the use of optically stimulated luminescence dosimeters (OSLDs) to monitor eye lens doses in the interventional environment is currently under analysis [13,18,19].

\* Corresponding author.

E-mail address: [luis.alejo@salud.madrid.org](mailto:luis.alejo@salud.madrid.org) (L. Alejo).

OSLDs have the advantage of high sensitivity, rapid readings and the ability to read the absorbed dose multiple times [20,21], features very useful for a medical physics department. Moreover, their high dependence on energy in the radiology range can be corrected [21] and its uncertainty taken into account [13,19]. In terms of paediatric IC eye lens dose measurements, some of these features (such as high sensitivity) might be particularly useful because paediatric patients present high morphological variability, with generally smaller thicknesses than adults, and these procedures are performed using equipment adjusted to low-dose rates [22,23].

To monitor the eye lens dose, the recommended operational quantity is  $H_p(3)$  [24,25], although there are currently no available conversion coefficients in international standards, and dosimeters designed for  $H_p(3)$  are not widely available [26]. A number of authors have recently attempted to provide air kerma-to- $H_p(3)$  conversion coefficients for RQR radiation qualities, typical for IC [27]. However, other authors have suggested that  $H_p(0.07)$  is sufficiently reliable for the photon energy involved in radiology and IC [18,26,28–30].

To assess the dose levels to the lens of the eye in paediatric IC prior to routine monitoring [30], a correlation study was performed comparing the eye lens dose estimations performed in terms of  $H_p(0.07)$  with nanoDot OSLDs placed next to the eyes of the only two paediatric interventional cardiologists working with a biplane system in the facility and the  $H_p(0.07)$  personal dose equivalent measured with whole body InLight OSLDs on the thorax, over the left side of their lead aprons. Moreover, the relationship between the dose to the cardiologists' lenses and the patient dose, in terms of kerma-area product ( $P_{KA}$ ) [31], was also analysed. The measurements were performed during interventions, on a monthly basis, from March 2014 to February 2015. Because the paediatric patients are usually small-sized and the procedures are complex, the use of a ceiling-suspended screen is often uncomfortable for correct work and is frequently disregarded. On the other hand, the nanoDots were placed on the external side of the cardiologists' lead goggles to hold them tightly in the vicinity of the left eye. Therefore, in this survey, no radiation protection devices were usually considered.

## 2. Materials and methods

### 2.1. Dosimeters, detectors and X-ray equipment

The dosimetry equipment used in this study consisted of a set of photo-luminescent crystal dosimeters called screened nanoDots (Landauer Inc<sup>1</sup>, IL, USA), an OSL reader (MicroStar, Landauer Inc.), an automatic annealer (InLight Annealer, Landauer Inc.) and an external PC with custom software. The nanoDots are composed of an active material ( $Al_2O_3:C$ ) measuring 4 mm in diameter and 0.3 mm thick, and they are covered with a  $10 \times 10 \times 2 \text{ mm}^3$  light-proof (when closed) plastic casing. InLight whole body OSLDs were also used in this study to obtain the personal dose equivalent over the aprons. InLight dosimeters are built with an  $83 \times 35 \times 15 \text{ mm}^3$  case, with metal and plastic filters, and a 4-position  $Al_2O_3:C$  detector slide component.

Prior to the eye lens dose measurements, the nanoDot dosimetry system was validated with irradiations performed using a general radiography unit (Digital Diagnost, Philips Healthcare) and a flat ionisation chamber (model 10x5-60) with a Radcal 9015 radiation meter (Radcal<sup>2</sup>, CA, USA). The ionisation chamber was calibrated by official calibration laboratories, and had an energy dependence lower than 5% for the energy range employed. The in-room IC

equipment was a Siemens Artis Zee VC14 biplane angiographic X-ray system, equipped with two 100-kW generators at 125 kV and 2 flat amorphous silicon detectors with caesium-iodide scintillators. The tube was a Megalix CAT Plus model (Siemens), tri-focus (0.3, 0.6 and 1 mm), with a  $12.5^\circ$  tungsten-rhenium anode and a 2.5 mm Al inherent filtration. This equipment typically uses the Cardio 3040 Siemens protocol, with 3 fluoroscopic modes (high-dose fluoroscopy FL3040<sup>+</sup>, normal fluoroscopy FL3040 and low-dose fluoroscopy FL3040<sup>-</sup>), and acquisition or cine (LV3040). A rotational 3-D acquisition or cone-beam computed tomography (CBCT) is also used (with a cardiac diagnostic protocol 5sDRc and a low-dose protocol 5sDR-L). The default fluoroscopy mode is 10 pulses per second ( $\text{ps}^{-1}$ ), although the two cardiologists (who are trained and certified in radiological protection according to national regulations) routinely use  $3 \text{ ps}^{-1}$  to reduce the patient dose when image quality is not a concern. In cine mode, the default configuration is 30 frames per second ( $\text{fs}^{-1}$ ), which is routinely used. The CBCT acquisition is performed with  $26.6 \text{ fs}^{-1}$  and a 5-s acquisition time. The characteristics of the evaluated X-ray beams were measured using a beam analyser detector calibrated for the energy under consideration (Unfors RaySafe Xi Base Unit and R/F detector<sup>3</sup>). The beam analyser has an uncertainty in half-value layer (HVL) measurements of less than 10% for the energy range employed. To collect all the workload data, including the  $P_{KA}$  values of both planes to study the correlation between patient and staff eye lens dose, the automatic dose management software CareAnalytics (Siemens) was used.

### 2.2. Dosimetry system validation, reading process and calibration

Prior to the measurement process, various tests were performed to validate the OSL dosimetric system: reproducibility, linear dose-response, signal depletion from readouts and lower detection limit. The first 3 tests were performed according to Al-Senan's procedure [21]. The lower detection limit (LD) was obtained according to Sonder et al. [32]. Dosimeter reproducibility was found to be between 0.8% and 1.3%, and good linearity between the nanoDot response and the ionisation chamber dose was obtained, with  $R^2$  higher than 0.99 ( $p < 0.05$ ). The correction factor  $d$  for decrease of signal per readout was found to be  $0.995 \pm 0.002$ . The lower detection limit in terms of  $H_p(0.07)$  was found to be  $16 \mu\text{Sv}$ . Lastly, and as part of the MicroStar reader's quality control (QC) procedure,<sup>4</sup> the reader's stability was tested every day before measurements, analysing the response of the photomultiplier tube after undergoing a stimulus from a set of light-emitting diodes, and with no stimulus present. The reader was considered stable if no response exceeded the corresponding mean and variance control limits [33,34].

The reading process consists of 5 successive readings, correcting each reading by the corresponding signal depletion  $f_d$ . The average of the last 4 readings was considered the best estimate of the cumulative counts in the dosimeter, and uncertainties in type A (due to the dispersion of the readings) and type B (due to the resolution and stability of the reader) were taken into account [35]. The best estimate of the counts obtained during a single irradiation,  $C$ , was considered to be the average counts after the exposure minus the average residual counts remaining after the annealing.

The system was calibrated in terms of *kerma* and  $H_p(0.07)$ , using 15 pre-irradiated nanoDots provided by the manufacturer, exposed to 5 air-kerma levels: 0 (unexposed), 3.37, 20.27, 337.83 and 675.67 mGy (uncertainty in the irradiation of 5%, coverage factor  $k = 2$ ). The beam quality used was RQR6 [36] (80 kVp, average energy 44 keV and HVL of 3.01 mm Al). The microStar reader

<sup>3</sup> <http://www.raysafe.com>.

<sup>4</sup> N. T. Ranger (2012) microStar Reader Quality Assurance Programme. <http://solutions.landauer.com/images/site/microstar/documents/microstar-quality-assurance-presentation.pdf>.

<sup>1</sup> <http://www.landauer.com>.

<sup>2</sup> <http://www.radcal.com>.

**Table 1**  
Reader calibration coefficients for RQR6.

Calibration	$N_{D,Q_0}$ (mGy(mSv)/counts)	$\Delta N_{D,Q_0}$ (%)
kerma (mGy)	$(1.41 \pm 0.03) \times 10^{-4}$	2
$H_p(0.07)$ (mSv)	$(2.13 \pm 0.04) \times 10^{-4}$	2

employs 2 calibrations: low and high dose. The LED beam operates in high-power mode for low doses and in low-power mode for high doses. Readings in this study were performed exclusively in the low-dose mode. The calibration coefficients, obtained in terms of *kerma* and  $H_p(0.07)$ , for the beam quality RQR6 are shown in Table 1. The calibration QC was performed using a different set of QC dosimeters provided by the manufacturer, according to the manufacturer's instructions.<sup>5</sup> Discrepancies with nominal doses of the QC calibration dosimeters were found to be approximately 1% in both *kerma* and  $H_p(0.07)$  calibrations.

### 2.3. Equivalent eye lens dose expression

For the measurements performed during interventions on cardiologists' goggles, the  $H_p(0.07)$  derived from the nanoDots dosimeters was calculated using the following expression:

$$H_p(0.07) = CN_{D,Q_0}Sk_{Q,Q_0}k_a, \quad (1)$$

where  $C$  are the accumulated counts obtained in the reading process;  $N_{D,Q_0}$  is the calibration coefficient in terms of  $H_p(0.07)$  obtained with an RQR6 quality beam; and  $S$  is the sensitivity correction factor of each screened nanoDot (provided by the manufacturer), with a nominal uncertainty of 2%. Finally,  $k_{Q,Q_0}$  and  $k_a$  are, respectively, the dosimeter's beam quality and angular response correction factors. The estimation of both factors and the evaluation of its uncertainties will be explained in detail in the following section. The uncertainty of the calibration coefficient was obtained by error propagation through the uncertainty of the irradiation of the calibrating dosimeters and the  $\Delta C_i$  readout uncertainties obtained in the calibrating process. The final  $H_p(0.07)$  uncertainty was obtained by error propagation in expression (1).

### 2.4. Angular and energy dependence analysis

Considering that the eye lens dosimeters were located on the external left side and in the centre of the cardiologists' goggles, it was difficult to determine the most probable angle of irradiation for all the procedures. Furthermore, the geometry (and energy) of the field of scattered radiation changed with time in each procedure. Therefore, we corrected for angularity by applying a correction factor that was the mean of the maximum and minimum response of the dosimeter, depending on the relative irradiation angle, for the image modalities typically employed by the paediatric cardiologists: the Cardio 3040 protocol, normal fluoroscopy (FL3040) and cine (LV3040). The setup of these measurements was as follows. As scatter, a  $20 \times 20 \times 12$  cm<sup>3</sup> polymethylmethacrylate (PMMA) slab was used. The table height was 103 cm, and the focus-detector distance was 95 cm in plane A. The detector-PMMA distance was 10 cm, and a 32-cm field of view (FOV) was selected. In normal fluoroscopy, the cardiologists typically used  $3 \text{ ps}^{-1}$ , although to optimise the time,  $30 \text{ ps}^{-1}$  was chosen. For LV3040 acquisition,  $30 \text{ fs}^{-1}$  was selected. Beam modality specifications corresponding to that experimental setup are shown in Table 2. The nominal kilovoltage peak (kVp), current (mA), automatic filter (mm Cu) and focus displayed by the equipment are

**Table 2**  
Beam modality specifications.

	FL 3040	LV 3040
kVp	65	73
mA	50	17
mm Cu	0.6	0
$\dot{K}_{a,i,rp}$ (mGy/min)	1	28
HVL (mm Al)	6.11	2.55
$E_{eff}$ (keV)	47	32
$E$ (keV)	50	44
FOV (cm)	32	32

shown. Nominal fluoroscopy and cine incident air kerma in reference point rates  $\dot{K}_{a,i,rp}$  (mGy/min) [31] are also reported. HVL was measured with the beam analyser detector on the PMMA slab, outside the sensitive region of the flat panel (~60% of the whole area). The effective photon energy  $E_{eff}$  (keV) for every beam quality was estimated using the experimental HVL values and the corresponding mass attenuation coefficients for aluminium [37]. Mean photon energies  $E$  (keV) were estimated using the spectrum calculator SPEKTR [38]. No collimation was used during these measurements.

To assess the maximum angular dependence of the nanoDots in the field of scattered radiation for the energies considered, 12 nanoDots were placed over the table in front of the  $20 \times 20 \times 12$  cm<sup>3</sup> PMMA slab at a distance of 80 cm and simultaneously irradiated, varying the position by 90° in each spatial direction by placing them on the faces of a box (see Fig. 1). An additional angle of 45° was used for consistency purposes. The  $k_a$  factors were obtained by comparing the dosimeter response in the reference orientation with the responses in the angled orientations. In the calculation of the uncertainty of this factor, a uniform distribution was considered.

As with the angular dependence analysis, significant variability in the scattered radiation field energy in interventional procedures was expected (changes in kV and added filtering in both tubes). Thus it was difficult to precisely define the most probable beam quality during interventions. Therefore, as with the angular dependence, we corrected for energy by averaging the maximum and minimum of the energy correction factors presented in a white paper by the manufacturer, Landauer Inc. [40], for the energy range considered. These factors were obtained through the relative response of nanoDots to RQR6 beam quality (Fig. 2). The exponential fit of the energy response is shown in the next equation:

$$Response = \exp \left[ \frac{a+cx+ex^2}{1+bx+dx^2+fx^3} \right] \quad (2)$$

$x$  = Mean energy (keV)

$$a = -0.599$$

$$b = -0.020$$

$$c = 0.026$$

$$d = 2.44e - 04$$

$$e = -2.44e - 04$$

$$f = -6.7e - 08$$

In this study, mean energies were considered from 29 keV, which can correspond to low kV acquisitions used in paediatric patients, up to 65 keV, which is typical of heavily filtered beams of low fluoroscopy [18]. Moreover, the low energy limit of 29 keV can correspond to RQR2 quality beams (40 kVp, 28.4 keV, 1.42 mm Al), and the upper energy limit to RQR10 (150 kVp, 64.3 keV, 6.57 mm Al) [36]. Thus, the average of the maximum and minimum energy correction factors obtained between 29 keV and 65 keV was considered. In the calculation of the uncertainty of the resultant beam quality correction factor, a uniform distribution was considered.

<sup>5</sup> Clifford J. Yahnke, Ph.D. Director of Technology (2009) Calibrating the microStar (<http://www.landauer.com>).

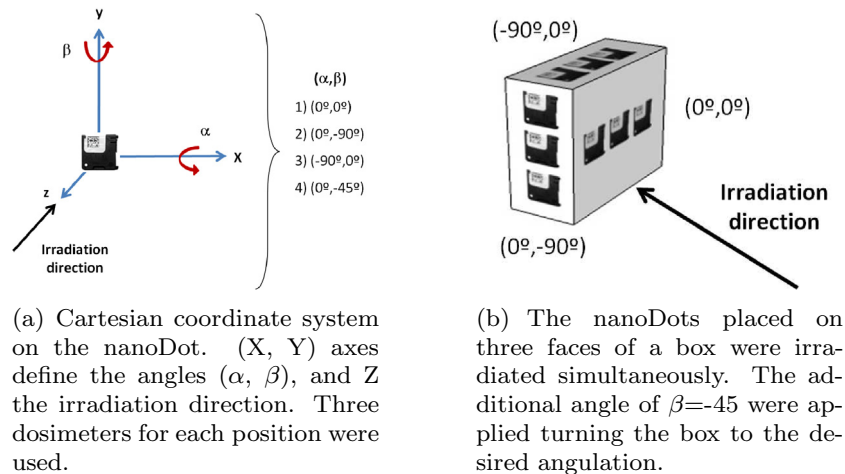


Fig. 1. Geometry used to assess the maximum angular dependence of the nanoDots.

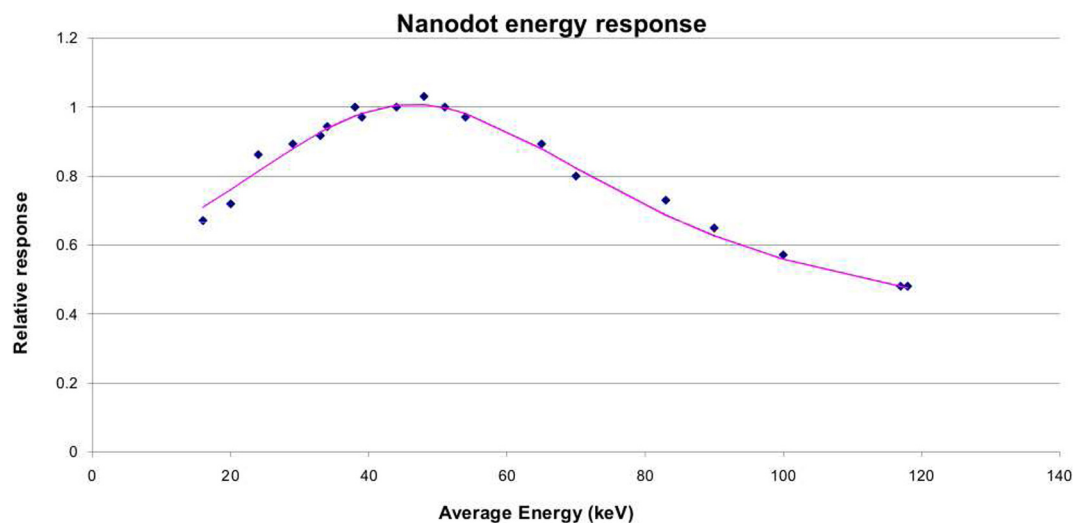


Fig. 2. The nanoDot energy response to RQR6 on  $30 \times 30 \times 15$  acrylic phantom. The inverse of the relative response is the energy correction factor  $k_{Q,Q_0}$ .

Finally, the minimum nanoDot signal with respect to the normal incidence was observed in fluoroscopy, with its edge oriented towards the scatter ( $90^\circ$ ), and was found to be  $0.82 \pm 0.03$ . Therefore, the corresponding maximum angular correction factor was  $1.22 \pm 0.02$ . On the other hand, the minimum and maximum energy correction factors given by the manufacturer, between 29 keV and 65 keV, was 0.97 and 1.12, respectively. Thus, the average of the maximum and minimum energy and angular correction factors was taken into account, and a uniform distribution was considered to obtain its uncertainties. In Table 3, the resulting angular and energy correction factors to the dose used in the eye lens dose estimations are shown.

Table 3  
Energy and angular correction factors to the eye lens dose.

Energy correction factor		Angular correction factor	
$k_{Q,Q_0}$	$\Delta k_{Q,Q_0}$	$k_a$	$\Delta k_a$
$1.05 \pm 0.04$	4%	$1.11 \pm 0.07$	7%

### 2.5. Eye lens dose estimates during interventions

The eye lens dose, in terms of  $H_p(0.07)$ , was estimated with nanoDot point dosimeters placed on the external side of the cardiologists' goggles during every diagnostic and therapeutic procedure performed over a 1-year period (from March 2014 to February 2015). The measurements were performed on a monthly basis: cardiologist 1 performed 109 procedures, and cardiologist 2 performed 113. Cardiologist 1 is approximately 180 cm tall and is relatively inexperienced (no more than 2 years). Cardiologist 2 is approximately 165 cm tall and is more experienced (over 20 years). The estimates of the eye lens dose were performed by placing 2 nanoDots on the external left side of the cardiologists' goggles and at the centre (Fig. 3). These 2 measurements (external left side and centre) were considered the bound values of the real left eye lens dose, and the mean the closest value, if the protection of the lead goggles is not taken into account. To obtain the uncertainty, a triangular distribution of these 2 measurements was considered, because there is reason to expect that the eye lens dose values within but close to the bounds are less likely than those nearer the centre of the bounds [35]. The quadratic sum of the

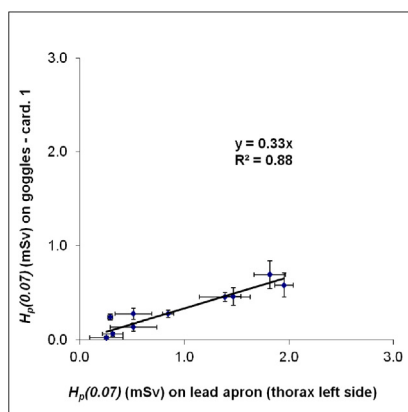


**Fig. 3.** OSLDs placed on the cardiologist's goggles, two on the external left side and two in the centre.

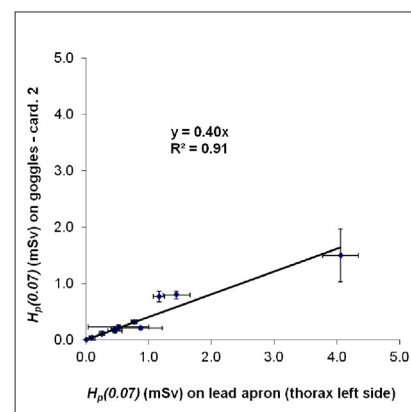
uncertainties of the two measurements was added as another type B uncertainty component to reflect the fact that the triangular distribution is not exact, because the bound values have its own uncertainty.

#### 2.6. Correlations between eye lens dose estimates, personal dose equivalent over the aprons and patient dose

Simultaneously with the nanoDots, a personal whole body InLight dosimeter was placed on the thorax, over the left side of the cardiologists' lead aprons, in order to determine the correlation between the  $H_p(0.07)$  personal dose equivalent and the left eye lens dose estimates. Readings were also made on a monthly basis, and the doses were compared. In the comparisons, the square of the Pearson coefficient was used.



(a) For cardiologist 1, the correlation between the eye lens dose estimates performed on the goggles and the personal dose equivalent measured at the left of the thorax on the lead apron, both in terms of  $H_p(0.07)$ .



(b) For cardiologist 2, the correlation between the eye lens dose estimates performed on the goggles and the personal dose equivalent measured at the left of the thorax on the lead apron, both in terms of  $H_p(0.07)$ .

**Fig. 4.** Results by cardiologist of the correlation between the eye lens dose estimates and the personal dose equivalent measured on the thorax.

To study the correlation between the estimate of the cardiologists' eye lens dose and the dose to the patient,  $P_{KA}$  readings using CareAnalytics were also performed on a monthly basis, including both cardiologists. The square of the Pearson coefficient was obtained in the comparisons. The  $P_{KA}$  meter was verified *in situ* using the calibrated ionisation chamber [41], and the values were corrected using the appropriate measured calibration factors to take into account the radiation attenuation by the table and mattress when Plane A was used. Calibration coefficients varied by  $\pm 15\%$ , with an uncertainty of less than 2%.

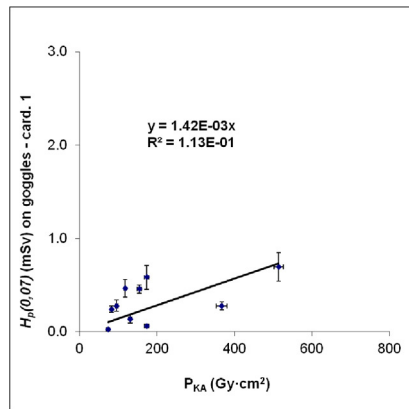
To compare the annual eye lens dose levels obtained with nanoDots and through the correlations with the personal dose equivalent and patient exposure, the uncertainties of the linear slopes and the Pearson coefficients were calculated using the Bootstrap method [39].

### 3. Results

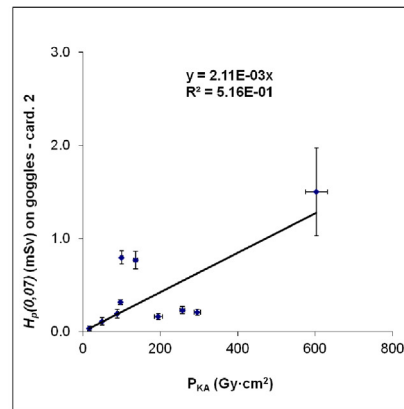
#### 3.1. Correlation studies

In Fig. 4(a), the correlations between the eye lens dose estimates in terms of  $H_p(0.07)$  measured on the goggles (average of centre and left side measurements), and the  $H_p(0.07)$  personal dose equivalent over the apron, on the left side of the thorax, is shown for cardiologist 1. In Fig. 4(b), the result is shown for cardiologist 2. For cardiologist 1, 10 readings made on a monthly basis were used; and 11 readings were used for cardiologist 2. The correlation for cardiologist 1 was  $R^2 = 0.88$ , and the ratio between the doses was 0.33. For cardiologist 2, the correlation was  $R^2 = 0.91$ , and the ratio between the doses was 0.40.

In Fig. 5(a), the correlations between the eye lens dose estimates, in terms of  $H_p(0.07)$  measured on the goggles (average of centre and left side measurements), and the dose to the patients obtained in terms of  $P_{KA}$ , is shown for cardiologist 1. In Fig. 5(b), the result is shown for cardiologist 2. For cardiologist 1, 10 readings made on a monthly basis were used, and 11 for cardiologist 2. The correlation for cardiologist 1 was  $R^2 = 0.11$ , and the ratio between the doses was  $1.42 \mu\text{Sv Gy}^{-1} \text{cm}^{-2}$ . For cardiologist 2, the correlation was  $R^2 = 0.52$ , and the ratio between the doses was  $2.11 \mu\text{Sv Gy}^{-1} \text{cm}^{-2}$ .

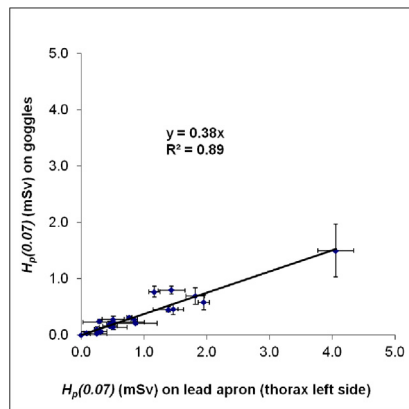


(a) For cardiologist 1, the correlation between the eye lens dose estimates performed on the goggles, in terms of  $H_p(0.07)$ , and the dose to the patients in terms of  $P_{KA}$ .

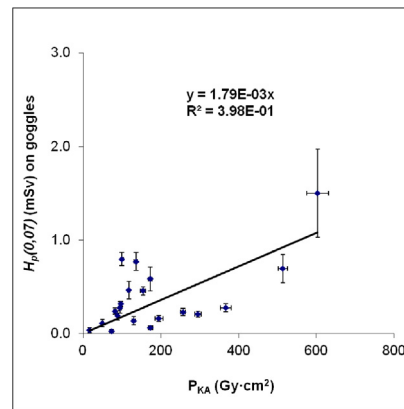


(b) For cardiologist 2, the correlation between the eye lens dose estimates performed on the goggles, in terms of  $H_p(0.07)$ , and the dose to the patients in terms of  $P_{KA}$ .

**Fig. 5.** Results by cardiologist of the correlation between the eye lens dose estimates and the dose to the patients.



(a) For both cardiologists, the correlation between the eye lens dose estimates performed on the goggles and the personal dose equivalent measured over the aprons, in terms of  $H_p(0.07)$



(b) For both cardiologists, the correlation between the eye lens dose estimates in terms of  $H_p(0.07)$  measured on the goggles and the  $P_{KA}$  provided by the equipment

**Fig. 6.** For both cardiologists, the results of the correlation studies between the eye lens dose estimates, the personal dose equivalent measured on the thorax and the dose to the patients.

Attending to the first operator position (and therefore considering both cardiologists), in Fig. 6(a) the correlation is shown between  $H_p(0.07)$  on the goggles and on the cardiologist's apron. In this study, 21 readings made on a monthly basis were used. The correlation was  $R^2 = 0.89$ , and the ratio between the doses was 0.38. In Fig. 6(b), the correlation is shown between  $H_p(0.07)$  on the goggles and the patient dose in terms of  $P_{KA}$ . In this study, 21 readings were made on a monthly basis (the same readings as Fig. 6(a) were considered for the eye lens dose estimates). The correlation obtained was  $R^2 = 0.40$ , and the ratio between the doses was  $1.79 \mu\text{Sv Gy}^{-1} \text{cm}^{-2}$ .

### 3.2. Dose per procedure and $H_p(0.07)/P_{KA}$

The personal dose equivalent per procedure in the first operator position, obtained with measurements performed over the aprons,

was  $102 \pm 16 \mu\text{Sv}$ . The eye lens dose per procedure estimated through measurements performed on the goggles was  $40 \pm 9 \mu\text{Sv}$ , and a patient dose per procedure of  $18 \pm 3 \text{Gy}\cdot\text{cm}^2$  was obtained. Therefore, the eye lens dose estimate in terms of  $H_p(0.07)$  normalized to  $P_{KA}$  was  $2.21 \pm 0.58 \mu\text{Sv Gy}^{-1} \text{cm}^{-2}$  ( $k = 2$  applied in all the cases of this section).

### 3.3. Annual eye lens dose estimates

In Table 4 the  $H_p(0.07)$  measurements made in a 1-year period on the left side and in the centre of the cardiologists' goggles with nanoDot dosimeters, and the personal dose equivalent measured over the left side of the cardiologists' lead aprons with whole body InLight dosimeters, are shown. In Table 5, the annual left eye lens dose estimates are shown, obtained averaging the goggles' left side

**Table 4**  
 $H_p(0.07)$  (mSv) annual measurements.

Cardiologist n°1			Cardiologist n°2		
On goggles		Over aprons	On goggles		Over aprons
Left side	Centre	Left side	Left side	Centre	Left side
4.94 ± 0.22	3.32 ± 0.16	10.83 ± 0.99	6.08 ± 0.33	3.89 ± 0.19	11.97 ± 1.44

**Table 5**  
 $H_p(0.07)$  (mSv) annual eye lens dose estimates.

Cardiologist n°1	Cardiologist n°2
4.13 ± 0.93	4.98 ± 1.28

and centre nanoDot values. In this section, a coverage factor of  $k = 2$  was applied in all the uncertainties.

In Fig. 7, a multiple comparison is shown between the annual estimate of the paediatric cardiologists' eye lens dose obtained with measurements performed on both cardiologists' goggles during interventions, the annual dose estimate obtained through the linear correlation between the eye lens dose estimate on the goggles and the personal dose equivalent on the thorax (see Fig. 6(a)), the annual dose estimate obtained through the linear correlation between the eye lens dose estimate on the goggles and the patient dose (see Fig. 6(b)), and finally the annual dose estimate obtained through the personal dose equivalent measured over the aprons, applying a reduction factor of 0.75 [42]. Given both cardiologists were evaluated in all the cases, these results correspond to the position of the first operator in paediatric IC. The red line shows the 6 mSv  $y^{-1}$  eye lens dose level proposed in July 2016 by the International Radiation Protection Association for implementation of regular dose monitoring with a collar or head dosimeter [30].

## 4. Discussion

### 4.1. Correlation studies

In Fig. 4(a) and (b), we can see a good correlation between the personal dose equivalent obtained over the aprons and the left eye lens dose estimates, both in terms of  $H_p(0.07)$ . However, the ratio between the doses was found to be far from 1. A similar result is found if we consider both cardiologists (and therefore, the first operator position, see Fig. 6(a)). The ratio eye lens/chest is similar to the eye lens/thyroid ratio obtained by Li et al. [43] in paediatric IC procedures, in which a value of 0.49 is slightly higher, possibly due to the fact that thyroid is nearer to the eyes than is the chest, and therefore the dose value measured by the thyroid dosimeter is closer to the eye lens dose value estimated in the eye's vicinity. However, both ratios are lower than the average relation of 0.75 between the eye lens dose and the  $H_p(10)$  dose measured with personal dosimeters placed on the upper left side of the torso, obtained by Lie et al. (2008) [42], and applied to Fig. 7. The ratios are also lower than the average relation of 0.7 between the  $H_p(3)$  eye dose and the  $H_p(10)$  dose measured on the left side of the chest, obtained by Farah et al. (2013) in IC procedures performed on adult patients [44]. Furthermore, the ratios are even lower than the relation of 0.6 between the  $H_p(0.07)$  eye lens doses obtained with OSLDs placed at the outer left side of cardiologists' goggles and

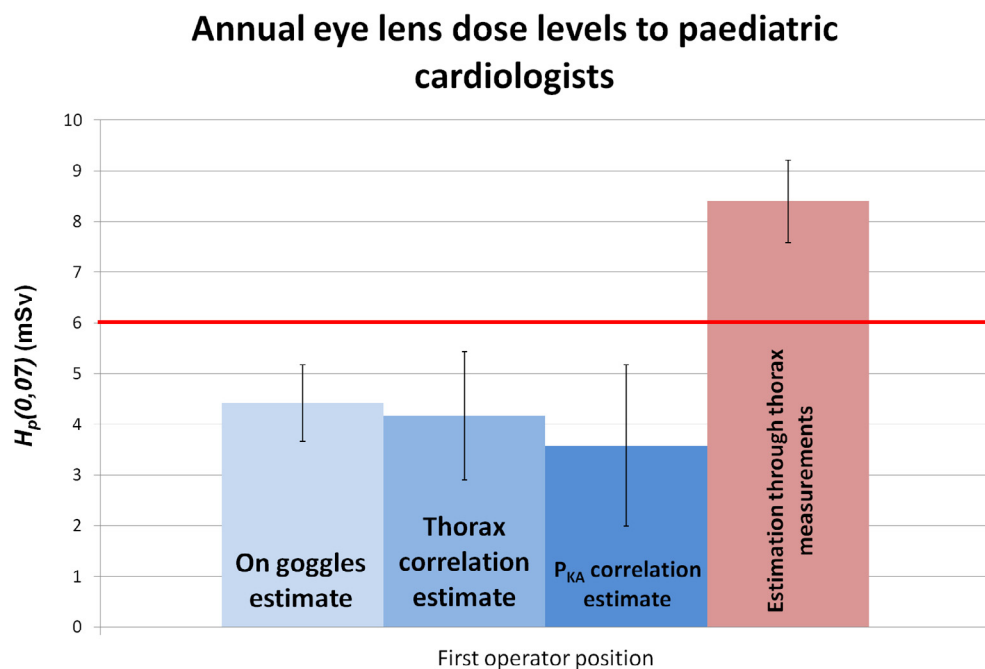


**Fig. 7.** Annual eye lens dose estimates to paediatric cardiologists in terms of  $H_p(0.07)$  obtained on the goggles and over the aprons (applying a reduction factor of 0.75). The estimates obtained through the linear correlations between the eye lens dose, the personal dose equivalent measured on the thorax and the  $P_{KA}$  are also shown. The red line shows the eye lens dose warning level of 6 mSv  $y^{-1}$ .

the  $H_p(10)$  doses over the chest apron readings from electronic dosimeters obtained by Sanchez et al. (2016), also in IC procedures on adult patients [7]. As indicated by Vanhavere et al. [45] and Sanchez et al. [7], the differences between  $H_p(0.07)$ ,  $H_p(3)$  and  $H_p(10)$  are of less importance for these beam qualities than the geometric position of the dosimeters. According to the inverse-square law, the scattered radiation field around the paediatric patient could have more gradient, compared with adults, because their size is typically smaller and the cardiologists are very close to the patient. This effect would explain the low eye lens/chest ratio obtained in this study compared with adult IC procedures. On the other hand, higher Pearson coefficients were obtained compared with the values of Sanchez et al. [7] and Principi et al. [6] (0.59 and 0.4, respectively). Given in paediatric IC performed with a biplane system the two X-ray tubes are often used simultaneously, and the CBCT contribution to the  $P_{KA}$  is not negligible [10], the scattered radiation around the patient could be more isotropic when compared with adult patients and mono-tube measurements. This effect would lead to a more uniform exposure for both eyes and whole-body dosimeters, explaining the high correlation coefficients obtained.

A poor correlation between dose to the patients, in terms of  $P_{KA}$ , and eye lens dose estimates for cardiologist 1 was observed (see Fig. 5(a)). For cardiologist 2, the Pearson correlation was moderate but statistically significant ( $p < 0.001$ , see Fig. 5(b)). However, if we take into account the first operator position (and therefore, the two cardiologists, see Fig. 6(b)), we obtain a correlation coefficient of  $R^2 = 0.40$ . This value is lower compared with the values of Principi et al. [6] and Antic et al. [46] (0.6 and 0.68, respectively). As noted by Antic et al., the correlation between the eye dose and  $P_{KA}$  strongly depends on the use of collective radiation protection tools. Given in paediatric IC the use of ceiling-suspended screen is not usually kept constant (due to the complexity of procedures), this effect could explain the poor relationship between the eye dose and the kerma-area product provided by the linear regression.

#### 4.2. Dose per procedure and $H_p(0.07)/P_{KA}$

Table 6 presents the eye lens dose estimates and the  $P_{KA}$  per procedure, as well as the eye lens dose estimates normalized to the  $P_{KA}$  for the first operator, compared with the results of similar studies (mean values). The  $P_{KA}$  per procedure obtained in this study is the lowest, possibly due to the typically smaller-sized patients compared with adults and to the fact that the equipment is dose-optimised for paediatric IC [22]. The eye lens dose value obtained is also the lowest, possibly for the same reason. However, the eye lens dose normalized to the  $P_{KA}$  is the highest. This result could be due to the fact that in paediatric IC the ceiling-suspended screen is often disregarded because it is uncomfortable for performing the procedure correctly. The eye lens dose mean value for paediatric IC published by Principi et al. is much greater compared with the value obtained in this study. Because the normalized value is

**Table 6**

Comparison of published data on eye lens dose estimates and the eye lens dose estimates normalized to the  $P_{KA}$  for interventional cardiology procedures for the first operator.  $P_{KA}$  values per procedure are also shown for discussion purposes.

	Eye lens dose ( $\mu\text{Sv}$ )	Eye lens dose/ $P_{KA}$ ( $\mu\text{Sv Gy}^{-1} \text{cm}^{-2}$ )	$P_{KA}$ ( $\text{Gy cm}^2$ )
Vanhanere et al. [45]	57	1.0	–
Antic et al. [46]	121 ± 84	0.94 ± 0.61	157 ± 126
Principi et al. [6]	171 ± 83 <sup>a</sup>	1.81	–
Vano et al. [47]	50 ± 104	0.84 ± 1.65 <sup>b</sup>	96 ± 79
This study	40 ± 9	2.21 ± 0.58	18 ± 3

<sup>a</sup> This value is obtained for paediatric interventions.

<sup>b</sup> This value is obtained with dosimeters worn over the aprons.

similar, we can assume the  $P_{KA}$  per procedure is much higher. This result could be explained if the X-ray systems used were dose-optimised for adult patients. However, more information is needed regarding the height of the cardiologist, his experience and the type of procedures performed.

#### 4.3. Annual eye lens dose estimates and comparisons

Higher annual doses for cardiologist 2 were obtained in all the measurements performed (see Table 4), mainly due to his shorter height, since a little difference of 5% in  $P_{KA}$  values is observed (and therefore similar workload was delivered). On the other hand, the doses were 49%–56% higher on the left side of the goggles than in the centre. This result is probably due to the irradiation geometry most commonly used during interventions (the patient is placed on the left side of the operator). As expected, the annual personal dose equivalent obtained with whole body InLight dosimeters placed on the left side of the cardiologists' aprons were the highest values for both cardiologists. With these measurements performed in-room during interventions over a 1-year period, the results of the previous phantom simulation published by Alejo et al. [13] are confirmed: all the doses obtained were below  $20 \text{ mSv y}^{-1}$ . Considering the eye lens dose per procedure estimated for the first operator position,  $40 \mu\text{Sv}$ , the annual eye lens dose limit can be reached with a workload of  $\sim 500$  procedures  $\text{y}^{-1}$ . This value is much higher than the 160 procedures  $\text{y}^{-1}$  reported by Antic et al. [46] in IC on adult patients, higher than the 400 procedures  $\text{y}^{-1}$  mean value reported by Vano et al. [47] and slightly lower than the 550 procedures  $\text{y}^{-1}$  reported by Sanchez et al. [7] (although in our survey the ceiling-suspended screen was not usually used). If we consider the attenuation of goggles, doses to the eye lenses could be reduced by a factor ranging from 2 to 7, depending on the irradiation geometry and the design of the glasses [48–50].

In Fig. 7, we see that the annual eye lens dose estimate through the personal dose equivalent measured over the aprons, obtained by applying the more commonly accepted reduction factor of 0.75, surpasses the  $6 \text{ mSv y}^{-1}$  warning level. Therefore, if we take into account only this estimation, regular eye lens dose monitoring performed with dosimeters placed next to the cardiologists' eyes is needed. However, the annual eye lens dose estimate obtained through measurements performed on goggles during interventions shows that regular monitoring next to the eyes is not needed. Moreover, noting the uncertainties, the estimate performed through the correlation with the personal dose equivalent is compatible with the estimate on the goggles. The annual eye lens dose obtained by the correlation with the  $P_{KA}$ , however, can underestimate the real value of the annual eye lens dose.

#### 4.4. Limitations of the study

Despite the large number of procedures evaluated in the 1-year period, the main limitation of this study is the low number of cardiologists submitted to dose assessment from a single installation (only two paediatric cardiologists were working in the facility when this study was performed). This limitation could lead to results that might not have general value, due to the large variability of the procedure protocols between facilities and the possibly different setups of radiology equipment.

## 5. Conclusions

An analysis has been performed of the correlations between the eye lens dose estimates performed with OSL dosimeters placed next to the eyes of two paediatric interventional cardiologists

working with a biplane system, the personal dose equivalent measured over their aprons and the patient dose obtained in terms of  $P_{KA}$ . The  $H_p(0.07)$  personal dose equivalent measured by the chest dosimeter has been found to be a good estimator of the  $H_p(0.07)$  eye lens dose, with good correlation, although with a low eye lens/chest ratio. A low correlation was found with the patient dose, although statistically significant. Per procedure, the  $P_{KA}$  and the eye lens dose estimates were much lower than the values reported in the literature for IC on adult patients; however, the eye lens dose value normalized to the patient dose was higher. This outcome highlights that the regular use of radiation protection tools could be optimised; in particular, the ceiling-suspended screen, which is often disregarded. Finally, the annual eye lens dose estimates obtained with the dosimeters placed on the goggles and from the linear regressions were all below  $6 \text{ mSv y}^{-1}$ ; therefore, no regular monitoring with collar or head dosimeter is needed.

## 6. Funding

This study was supported by the Spanish Nuclear Safety Council (*Consejo de Seguridad Nuclear*).

## References

- [1] United Nations Scientific Committee on the Effects of Atomic Radiation Sources and Effects of Ionizing Radiation, 2008, Report to the General Assembly with Scientific Annexes, 1, Sources United Nations, New York.
- [2] Dowling A, Gallagher A, O'Connor U, Larkin A, Gorman D, Gray L, Malone J. Acceptance testing and QA of interventional cardiology systems. *Radiat. Prot. Dosim.* 2008;129:291–4.
- [3] International Commission on Radiological Protection, ICRP Statement on Tissue Reactions, ICRP Publication 118, Ann. ICRP41(1/2), 2012.
- [4] Official Journal of the European Union, Council Directive 2013/59/EURATOM of 5 December 2013, L 13 de 17/01/2014, 2013, 1–73.
- [5] Vano E, Gonzalez L, Fernandez JM, Haskal ZJ. Eye lens exposure to radiation in interventional suites: caution is warranted. *Radiology* 2008;248(3):945–53. <http://dx.doi.org/10.1148/radiol.2482071800>.
- [6] Principi S, Delgado Soler C, Ginjaume M, Beltran Vilagrana M, Rovira Escutia JJ, Duch MA. Eye lens dose in interventional cardiology. *Radiat. Prot. Dosim.* 2015;165(1–4):289–93. <http://dx.doi.org/10.1093/rpd/ncv051>.
- [7] Sánchez RM, Vano E, Fernandez JM, Pifarre X, Ordiales JM, Rovira JJ, Carrera F, Goicolea J, Fernandez-Ortiz A. Occupational eye lens doses in interventional cardiology. A multicentric study. *J. Radiol. Prot.* 2016;36(1):133–43.
- [8] Ubeda C, Vano E, Miranda P, Leyton F. Pilot program on patient dosimetry in pediatric interventional cardiology in Chile. *Med. Phys.* 2012;39:2424–30.
- [9] Glatz AC, Patel A, Zhu X, Dori Y, Hanna BD, Gillespie MJ, Rome JJ. Patient radiation exposure in a modern, large-volume, pediatric cardiac catheterization laboratory. *Pediatr. Cardiol.* 2014;35:870–80.
- [10] Corredoira E, Vañó E, Ubeda C, Gutiérrez-Larraya F. Patient doses in paediatric interventional cardiology: impact of 3D rotational angiography. *J. Radiol. Prot.* 2015;35(1):179–95. <http://dx.doi.org/10.1088/0952-4746/35/1/179>.
- [11] Ubeda C, Vano E, Miranda P, Aguirre D, Riquelme N, Guarda E. Comparison of two angiographic systems in paediatric interventional cardiology. *Radiat. Prot. Dosim.* 2015;165(1–4):250–3. <http://dx.doi.org/10.1093/rpd/ncv035>.
- [12] Vano E, Ubeda C, Miranda P, Leyton F, Duran A, Nader A. Radiation protection in pediatric interventional cardiology: an IAEA pilot program in Latin America. *Health Phys.* 2011;101(3):233–7. <http://dx.doi.org/10.1097/HP.0b013e3182135fd1>.
- [13] Alejo L, Koren C, Ferrer C, Corredoira E, Serrada A. Estimation of eye lens doses received by pediatric interventional cardiologists. *Appl. Radiat. Isot.* 2015;103:43–7. <http://dx.doi.org/10.1016/j.apradiso.2015.05.008>.
- [14] Ubeda C, Vano E, Miranda P, Aguirre D, Riquelme N, Dalmazzo D, Galaz S. Patient and staff doses in paediatric interventional cardiology derived from experimental measurements with phantoms. *Phys. Med.* 2016;32(1):176–81.
- [15] International Commission on Radiological Protection. Avoidance of radiation injuries from medical interventional procedures, ICRP Publication 85, Ann. ICRP30(2), 2000.
- [16] Bilski P et al. The new EYE-D dosimeter for measurements of Hp(3) for medical staff. *Radiat. Meas.* 2011;46:1239–42.
- [17] Principi S, Ginjaume M, Duch MA, Sánchez RM, Fernández JM, Vano E. Influence of dosimeter position for the assessment of eye lens dose during interventional cardiology. *Radiat. Prot. Dosim.* 2015;164(1–2):79–83. <http://dx.doi.org/10.1093/rpd/ncv359>.
- [18] Sanchez RM, Vano E, Fernandez JM, Ginjaume M, Duch MA. Measurements of eye lens doses in interventional cardiology using OSL and electronic dosimeters. *Rad. Prot. Dosim.* 2014;162(4):569–76.
- [19] L. Alejo et al., Estimated radiation dose to the eye lens with photoluminescence dosimeters, International Atomic Energy Agency, IAEA-CN-223-171, 2014.
- [20] Chester SR. The energy dependence and dose response of a commercial optically stimulated luminescence detector for kilovoltage photon, megavoltage photon, and electron, proton, and carbon beams. *Med. Phys.* 2009;36(5):1690–9.
- [21] Al-Senan RN, Hatab MR. Characteristics of an OSLD in the diagnostic energy range. *Med. Phys.* 2011;38(7):4396–405.
- [22] Corredoira E, Vano E, Alejo L, Ubeda C, Gutierrez-Larraya F, Garayoa J. Biplane interventional pediatric system with cone-beam CT: dose and image quality characterization for the default protocols. *J. Appl. Clin. Med. Phys.* 2016;17(4).
- [23] Vano E, Ubeda C, Leyton F, Miranda A. Radiation dose and image quality for pediatric interventional cardiology. *Phys. Med. Biol.* 2008;53(15):4049–62.
- [24] International Commission on Radiation Units and Measurements. Quantities and Units in Radiation Protection Dosimetry. ICRU Publications; 1993. ICRU Report 51 (ICRU Inc, Bethesda, MD, USA).
- [25] Carinou E, Ferrari P, Ciraj-Bjelac O, Ginjaume M, Sans-Merce M, O'Connor U. Eye lens monitoring for interventional radiology personnel: dosimeters, calibration and practical aspects of Hp(3) monitoring. A 2015 review. *J. Radiol. Prot.* 2015;35:R17–34. <http://dx.doi.org/10.1088/0952-4746/35/3/R17>.
- [26] TECDOC No. 1731. Implications for Occupational Radiation Protection of the New Dose Limit for the Lens of the Eye. Vienna: International Atomic Energy Agency, 2013. (IAEA-TECDOC series, ISSN 1011-4289; no. 1731) ISBN 978-92-0-115213-8.
- [27] Principi S, Guardiola C, Duch MA, Ginjaume M. Air kerma to Hp(3) conversion coefficients for IEC 61267 RQR X-ray radiation qualities: Application to does monitoring of the lens of the eye in medical diagnostic. *Radiat. Prot. Dosim.* 2015. pii: ncv435.
- [28] Behrens R, Engelhardt J, Figel M, Hupe O, Jordan M, Seifert R. Hp(0.07) photon dosimeters for eye lens dosimetry: calibration on a rod vs. a slab phantom. *Radiat. Prot. Dosim.* 2012;148(2):139–42.
- [29] International Commission on Radiological Protection, The 2007 recommendations of the International Commission on Radiological Protection. ICRP Publication 103, Ann. ICRP41(1/2), 2012.
- [30] International Radiation Protection Association, IRPA guideline protocol for eye dose monitoring and eye protection of workers. Document prepared by the IRPA TG on the impact of the Eye Lens Dose Limits, 2016. <http://www.irpa.net/page.asp?id=54696>.
- [31] International Commission on Radiological Units and Measurements. Patient dosimetry for X rays used in medical imaging. ICRU report 74. *J. ICRU* 2005;5(2):1–113.
- [32] E. Sonder et al., Background radiation accumulation and lower detection limit of detection in thermoluminescent beta-gamma dosimeters used by the centralized external dosimetry system. Office of Radiation Protection, 1991.
- [33] J.S. Oakland, Statistical Process Control, Butterworth Heinemann, fifth edition. ISBN-13: 978-0750669627 ISBN-10: 0750669624, 2003.
- [34] López-Tarjuelo J et al. Statistical process control for electron beam monitoring. *Physica Med.* 2015;31:493–500. <http://dx.doi.org/10.1016/j.ejmp.2015.05.006>.
- [35] Guide to the expression of uncertainty in measurement, 1° Ed. International standardization Organization (ISO). Geneva, Switzerland, 1995.
- [36] International Electro Technical Commission (IEC) Medical Diagnostic X-Ray Equipment—Radiation Conditions for Use in the Determination of Characteristics. 61267 Ed. 2.0. IEC, 2005.
- [37] Birch R, Marshall M, Ardan GM. Catalogue of spectral data for diagnostic X-rays. Hospital physicists association. *Sci. Rep. Ser.* 1979;30.
- [38] Siewerdsen JH et al. SPEKTR: A computational tool for X-ray spectral analysis and imaging system optimization. *Am. Assoc. Phys. Med.* 2004;31(11).
- [39] Bradley Efron. The Jackknife, the Bootstrap, and Other Resampling Plans (CBMS-NSF Regional Conference Series in Applied Mathematics), 1982. Society for Industrial and Applied Mathematics. ISBN-13:978-0898711790; ISBN-10:0898711797.
- [40] C.J. Yahnke, R.D. Hanify, M.R. Salasky, Microstar Calibration Conversion Factors for DOTs. MicroSTAR v2.0 User Manual. Available from Landauer, Inc. 2 Science Road, Glenwood, IL 60425, 2008. <http://solutions.landauer.com/images/site/microstar/documents/>.
- [41] IAEA. TRS457 International Atomic Energy. Dosimetry in Diagnostic Radiology: an International Code of Practice (Technical Report Series no. 457). Vienna: International Atomic Energy Agency; 2007.
- [42] Lie Ø, Paulsen GU, Wøhni T. Assessment of effective dose and dose to the lens of the eye for the interventional cardiologist. *Rad. Prot. Dosim.* 2008;132:313–8. <http://dx.doi.org/10.1093/rpd/ncn296>.
- [43] Li LB, Kai M, Takano K, Ikeda S, Matsuura M, Kusama T. Occupational exposure in pediatric cardiac catheterization. *Health Phys.* 1995;69:261–4.
- [44] Farah J, Struelens L, Dabin J, Koukorava C, Donadille L, Jacob S, Schnelzer M, Auvinen A, Vanhavere F, Clairand I. A correlation study of eye lens dose and personal dose equivalent for interventional cardiologists. *Radiat. Prot. Dosim.* 2013;157:561–9.
- [45] Vanhavere F et al. Measurements of eye lens doses in interventional radiology and cardiology: final results of the ORAMED project. *Radiat. Meas.* 2011;46(11):1243–7.
- [46] Antic V, Ciraj-Bjelac O, Rehani M, Aleksandric S, Arandjic D, Ostojic M. Eye lens dosimetry in interventional cardiology: results of staff dose measurements and link to patient dose levels. *Radiat. Prot. Dosim.* 2013;154:276–84.

- [47] Vano E, Sanchez RM, Fernandez JM. Estimation of staff lens doses during interventional procedures. Comparing cardiology, neuroradiology and interventional radiology. *Rad. Prot. Dosim.* 2015;165(1–4):279–83. <http://dx.doi.org/10.1093/rpd/ncv049>.
- [48] van Rooijen BD et al. Efficacy of radiation safety glasses in interventional radiology. *Cardiovasc. Intervent. Radiol.* 2014;37:1149–55.
- [49] Koukorava C, Farah J, Struelensm L, Clairand I, Donadille L, Vanhavere F, Dimitriou P. Efficiency of radiation protection equipment in interventional radiology: a systematic Monte Carlo study of eye lens and whole body doses. *J. Radiol. Prot.* 2014;34(3):509–28. <http://dx.doi.org/10.1088/0952-4746/34/3/509>.
- [50] Martin Colin J. Eye lens dosimetry for fluoroscopically guided clinical procedures: practical approaches to protection and dose monitoring. *Rad. Prot. Dos.* 2016;169(1–4):286–91. <http://dx.doi.org/10.1093/rpd/ncv431>.